

Landau-Zener transition rates of superconducting qubits and absorption spectrum in quantum dots

Jorge G. Russo^{1,2,*} and Miguel Tierz^{3,†}

¹*Institució Catalana de Recerca i Estudis Avançats (ICREA),*

Pg. Lluís Companys, 23, 08010 Barcelona, Spain

²*Departament de Física Cuàntica i Astrofísica and Institut de Ciències del Cosmos,*

Universitat de Barcelona, Martí Franquès, 1, 08028 Barcelona, Spain

³*Departamento de Análisis Matemático y Matemática Aplicada,*

Universidad Complutense de Madrid, 28040 Madrid, Spain

New exact formulas are derived for systems involving Landau-Zener transition rates and for absorption spectra in quantum dots. These rectify previous inaccurate approximations utilized in experimental studies. The exact formulas give an explicit expression for the maxima and minima of the transition rate at any oscillating period and reveal a number of striking physical consequences, such as the suppression of oscillations for half-integer values of the detuning parameter and that the periodic dependence on the detuning parameter changes at special values of the driving field amplitude. The fluorescence spectra of quantum dots exhibit similar properties.

I. INTRODUCTION

The production of a coherent superposition between quantum states in nanoelectronic circuits is one of the cornerstones for the development of quantum technology [1]. A distinguished example of this is the Landau-Zener-Stückelberg-Majorana (LZSM) interferometry [2, 3], which formerly was also simply known as Landau-Zener interferometry. The LZSM theory, was first developed around 1932 in the context of the study of spin dynamics and slow atomic collisions, demonstrated that transitions are possible between two approaching levels as a control parameter is swept across the point of minimum energy splitting. For a detailed account of all the different aspects and nuances of the first four seminal contributions, see [3–6].

In LZSM interferometry, a quantum two-level system is driven strongly across an avoided energy-level crossing producing first a quantum superposition between the two states of the

* jorge.russo@icrea.cat

† mtierz@ucm.es

system. The temporal evolution of the two states occurs with different dynamical phases and, after a second passage through the anticrossing, coherent interference between these two states occurs. A periodically driven field can also induce coherent Rabi oscillations for a different regime of parameters. Rabi oscillations occur when the driving frequency $\nu = \omega/2\pi$ is of the same order as the energy-level separation $\Delta E/\hbar$. The rate equation-based description, where transitions occur through the Landau-Zener effect, arises at $\hbar\nu \ll \Delta E$ and strong driving amplitude $A \sim \Delta E$ (for discussions, see [3, 7]).

There is an analogy between LZSM interferometry and Mach-Zehnder interferometry since the beamsplitters can be realized by Landau-Zener (LZ) transitions at a level avoided crossing and, over one oscillation period of the driving field, the qubit is swept through the avoided crossing twice. This point of view is developed in, for example, [3, 8] and it is applicable to settings discussed below, such as the double-passage setting (which is related to optical Mach-Zehnder [3]).

LZSM interferometry has been studied in a number of platforms. In the first part of this paper, we will be focusing on works where the platform is based on superconducting Josephson junctions [7, 9] (see also [10]). These works are characterized by the presence of noise but Landau-Zener transitions in externally driven systems have been considered, for example, also under dissipation [11, 12] or in the context of other mesoscopic systems [13].

We shall thoroughly reanalyze the transition rate in [7, 9], providing an exact analytical expression for it as well as an improved asymptotic characterization of the rate, which will include a more accurate portrayal of the oscillations with full analytical control.

The mathematical formula describing the LZSM transition rate also appears in the study of the absorption spectrum of quantum dots, with a reinterpretation of the parameters. In the second part we shall examine settings involving various external fields. An example consists in a system describing the dipole coupling of the quantum dot to a laser field. Concretely, we consider InAs/GaAs quantum dots (nanoscale islands of InAs embedded in a GaAs matrix) studied in [14] and study the absorption spectrum for two different configurations.

We shall also study the two-level system with modulated laser light discussed in [15], which appeared prior to the discovery of quantum dots, but it is nevertheless governed by related physics. Finally, we will examine the power spectrum of quantum dots in presence of a bichromatic electromagnetic field, investigated in [16], which is expressed as an infinite series of Mollow triplets [17]. Here the corresponding infinite sums will be computed analytically.

II. ANALYSIS OF THE TRANSITION RATE

Consider the two-level system (TLS) studied in [7] of a periodic driving on a qubit, with Hamiltonian

$$\mathcal{H} = -\frac{1}{2} \begin{pmatrix} h(t) & \Delta \\ \Delta & -h(t) \end{pmatrix}, \quad (1)$$

where $h(t) = \mathcal{E} + \delta\mathcal{E}(t) + A \cos \omega t$ is the energy detuning (or bias) from an avoided crossing, modulated by the driving field. The term $\delta\mathcal{E}(t)$ describes classical noise and Δ is the energy gap between the two levels. The LZ transition rate was computed in perturbation theory in [7], with the result

$$W = \frac{\Delta^2}{2} \sum_{n=-\infty}^{\infty} \frac{\Gamma_2 J_n^2(x)}{(\mathcal{E} - \omega n)^2 + \Gamma_2^2}, \quad x \equiv \frac{A}{\omega}, \quad (2)$$

where J_n is the Bessel function of the first kind. Note the symmetry property $W(-\mathcal{E}) = W(\mathcal{E})$. The parameter \mathcal{E} is the energy bias and Γ_2 is the decoherence rate [3, 7]¹.

The sum in equation (2) is usually evaluated numerically. However, attempts have been made to provide analytic approximations, as analytic formulas can reveal properties that are difficult to identify using numerical methods with generic parameters. In particular, in [7], and later on in [3, 18], this sum was computed by assuming that the main contributions come from large n terms, one can replace

$$J_n(x) \approx a \text{Ai}[a(n-x)], \quad a = (2/x)^{1/3}. \quad (3)$$

This approximation works well for a few oscillations but then the two functions $J_n(x)$ and $a \text{Ai}[a(n-x)]$ get out of phase.

The assumption that the main contributions come from large n terms requires that $\mathcal{E} \gg \omega$, so that the sum is dominated by terms with $n \approx n_0 \equiv [\mathcal{E}/\omega]$.

In [7], the remaining sum was approximated by the following heuristic formula

$$W_{\text{app}} = \frac{\pi a^2 \Delta^2}{2\omega} \text{Im}[\cot(\pi\mu^*)] \text{Ai}^2\left[\frac{a}{\omega}(\mathcal{E} - A)\right], \quad \mu \equiv \frac{1}{\omega}(\mathcal{E} + i\Gamma_2). \quad (4)$$

A numerical comparison shows that this formula approximates the sum (2) provided

- $\frac{\mathcal{E}}{\omega} \approx \text{integer} \gg 1$.
- $\Gamma_2 \ll 1$.

¹ If the relaxation time T_1 is taken into account, the upper level occupation probability can be calculated as in [3] (see section 3.6 and Appendix B.4.2). The resulting expression (Eq. B.62 in [3]), the stationary solution of the rate equation, cannot be evaluated using our analytic formulas.

A comparison between the original expression (2) and the approximation (4) is shown in fig. 1. We see big deviations between W and W_{app} because in the figures \mathcal{E}/ω is not an integer. Since physically there is no reason for \mathcal{E}/ω to be an integer, generically W_{app} significantly deviates from the actual rate W . This evident deviation does not affect fig. 4 in [7], as the fits with experimental data in that figure have been carried out by means of a numerical evaluation of the sum (2).

At large A , one can use the asymptotic formula for the Airy function, giving

$$W_{\text{app}} \approx \frac{\Delta^2}{2x\omega} \text{Im}[\cot(\pi\mu^*)] \left(1 - \frac{\varepsilon}{x}\right)^{-\frac{1}{2}} \cos^2 \left[\frac{2\sqrt{2}}{3} x \left(1 - \frac{\varepsilon}{x} - \frac{\pi}{4}\right) \right]. \quad (5)$$

As will become clear in the following, this formula gives an incorrect asymptotic frequency.

The formula (4) reproduces some qualitative features of the actual rate W : in particular, W_{app} is very small for $A < \mathcal{E}$ (with $\mathcal{E} \gg \omega$), so transitions occur only for $A > O(\mathcal{E})$. The frequencies of oscillations are similar. But it should be noted that minima and maxima are very different and also oscillations get out of phase after a few periods. Importantly, W_{app} has an infinite number of zeroes as a function of x , but the exact W never vanishes for any finite Γ_2 and generic values of \mathcal{E} . The limit $\Gamma_2 \rightarrow 0$ will be discussed below.

We will now show that one can actually compute the sum (2) *exactly* and in closed form, using a summation formula derived in [19] (reviewed in the appendix). Consider in general $\mu = \mu_1 + i\mu_2$. We first split

$$\sum_n \frac{J_n(x)^2}{(n - \mu_1)^2 + \mu_2^2} = \frac{1}{2i\mu_2} \left(\sum_n \frac{J_n^2(x)}{n - \mu} - \sum_n \frac{J_n^2(x)}{n - \mu^*} \right). \quad (6)$$

Using the formula (A5) of the appendix we thus find

$$\sum_n \frac{J_n(x)^2}{(n - \mu_1)^2 + \mu_2^2} = -\frac{1}{2i\mu_2} \left(\frac{\pi}{\sin(\pi\mu)} J_\mu(x) J_{-\mu}(x) - \frac{\pi}{\sin(\pi\mu^*)} J_\mu^*(x) J_{-\mu}^*(x) \right). \quad (7)$$

or

$$\boxed{\sum_n \frac{J_n(x)^2}{(n - \mu_1)^2 + \mu_2^2} = -\frac{1}{\mu_2} \text{Im} \left(\frac{\pi}{\sin(\pi\mu)} J_\mu(x) J_{-\mu}(x) \right)} \quad (8)$$

where we used that $J_{\mu^*}(x) = J_\mu^*(x)$ for real x . Therefore

$$W = -\frac{\Delta^2}{2\omega} \text{Im} \left(\frac{\pi}{\sin(\pi\mu)} J_\mu(x) J_{-\mu}(x) \right). \quad (9)$$

A numerical check shows that indeed the formula (9) exactly reproduces the expression (2) given by the infinite sum.

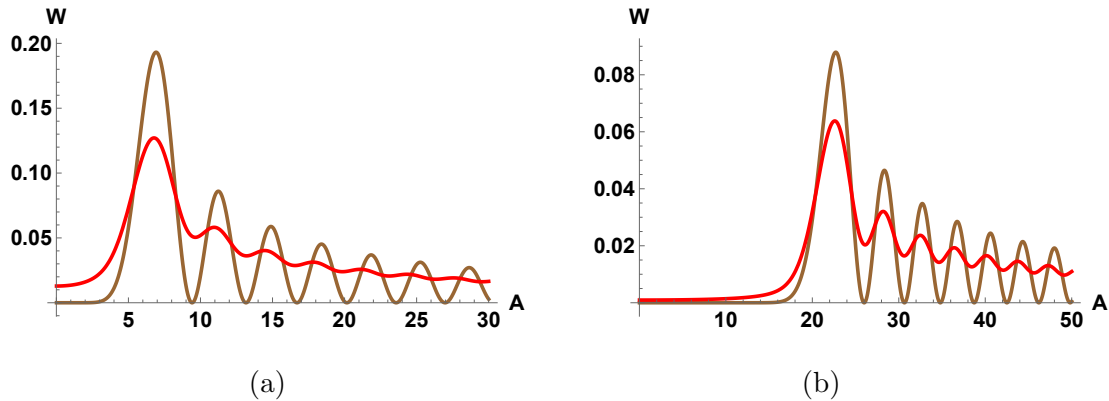


FIG. 1. (a) W (in units of Δ^2/ω) as a function of A (in units of ω). The approximation (4) (brown) vs. the exact formula (9) (red). Here $\mathcal{E} = 5.5\omega$, $\Gamma_2 = 5\omega/(2\pi)$. (b) $\mathcal{E} = 20.5\omega$, same value for Γ_2 .

Modulo an overall factor Δ^2/ω , W depends on three parameters (ε, γ, x) , with

$$\varepsilon \equiv \frac{\mathcal{E}}{\omega}, \quad \gamma \equiv \frac{\Gamma_2}{\omega}, \quad x \equiv \frac{A}{\omega}.$$

We can set $\omega = 1$ and plot the rate W as a function of A for different values of \mathcal{E} and Γ_2 , as in fig. 1. As noted above, the most notable difference is that the approximated transition rate (4) vanishes for specific values of x . This disagrees with the fact that the actual rate (2), (9) does not vanish anywhere for generic values of Γ_2 and \mathcal{E} .

The transition rate (2) exhibits an infinite set of resonances created by the driving force, which appear at integer values of the detuning ε . All resonances are encapsulated in the exact formula (9). Indeed, at the special values $\text{Re}[\mu] = n$, $n \in \mathbb{Z}$, one has

$$-\text{Im} \left(\frac{\pi}{\sin(\pi\mu)} J_\mu(x) J_{-\mu}(x) \right) = (-1)^n \frac{\pi}{\sinh(\pi\gamma)} \text{Re} [J_{n+i\gamma}(x) J_{-n-i\gamma}(x)] . \quad (10)$$

This shows that for integer ε the transition rate undergoes the expected enhancement at small γ ,

$$-\text{Im} \left(\frac{\pi}{\sin(\pi\mu)} J_\mu(x) J_{-\mu}(x) \right) \approx \frac{1}{\gamma} J_n^2(x) + O(\gamma), \quad (11)$$

a result that is also evident from the original formula (2), where the term $\mathcal{E} = \omega n$ dominates. This is in contrast with the behavior for generic (non-integer) values of ε , where the transition rate is proportional to γ .

Equation (11) shows that the height of the resonance peak is proportional to $J_n^2(x)$ and is therefore a function of the amplitude $A = x\omega$. For special values of the amplitude where the $J_n(x)$ has a zero, the peak at the detuning value $\varepsilon = \text{Re}[\mu] = n$ disappears, but other peaks with $\varepsilon = n'$, with $n' \neq n$ remain. Since the Bessel function possesses an infinite number of zeroes, it is apparent that there are infinite special values of amplitude where the peak at any given detuning $\varepsilon = n$ is suppressed.

Equation (11) also clarifies that the transition rate may have zeroes under two conditions: $\gamma \rightarrow 0$ and integer ε . In these cases, the zeroes of the (rescaled) transition rate γW coincide with the zeroes of the Bessel function $J_n(x)$.

A simple formula for W can also be given for large x , where one has the well known Bessel asymptotics [20],

$$J_\mu(x) \approx \frac{\sqrt{2}}{\sqrt{\pi x}} \cos\left(x - \mu\frac{\pi}{2} - \frac{\pi}{4}\right), \quad x \gg \text{Max}\{1, |\mu|^2\}. \quad (12)$$

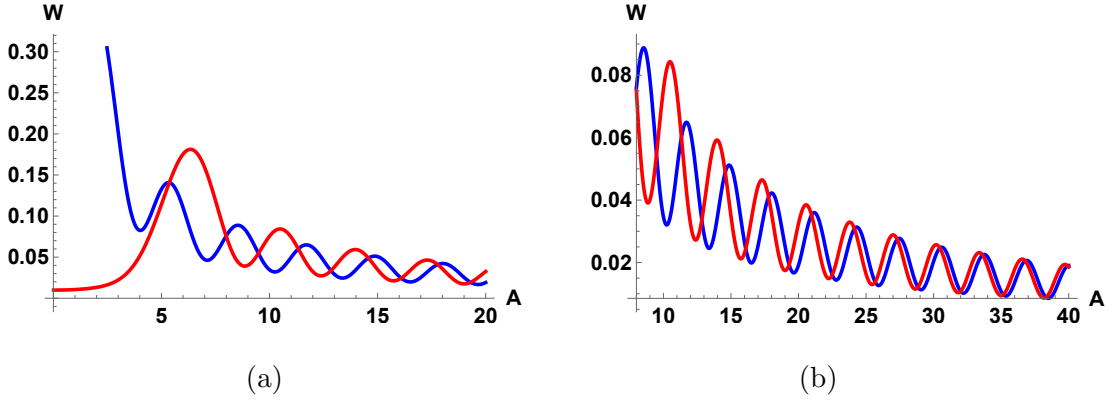


FIG. 2. At large amplitudes, the behavior of the transition rate is governed by the simple asymptotic behavior of the Bessel functions (red and blue colors correspond to W and W_{asym}). Here $\varepsilon = 5$, $\gamma = 0.5$, and W is given in units of Δ^2/ω . (a) At small x , one can see a gap due to the well known turning point of the Bessel functions around $x \sim |\mu|$ (*i.e.* $A \sim \mathcal{E}$). (b) When $x \gg |\mu|^2$, the asymptotic formula approaches the exact result.

Thus, for large x

$$-\text{Im} \left(\frac{\pi}{\sin(\pi\mu)} J_\mu(x) J_{-\mu}(x) \right) \approx -\frac{1}{x} \text{Im} \left(\frac{\cos(\pi\mu) + \sin(2x)}{\sin(\pi\mu)} \right). \quad (13)$$

Computing the imaginary part, we find

$$-\text{Im} \left(\frac{\pi}{\sin(\pi\mu)} J_\mu(x) J_{-\mu}(x) \right) \approx \frac{2}{x} \frac{\sinh(\pi\gamma)}{\cosh(2\pi\gamma) - \cos(2\pi\varepsilon)} (\cosh(\pi\gamma) + \cos(\pi\varepsilon) \sin(2x)). \quad (14)$$

Thus

$$W_{\text{asym}} = \frac{\Delta^2}{x\omega} \frac{\sinh(\pi\gamma)}{\cosh(2\pi\gamma) - \cos(2\pi\varepsilon)} (\cosh(\pi\gamma) + \cos(\pi\varepsilon) \sin(2x)), \quad (15)$$

which is clearly different from (4), (5). This formula explicitly shows the correct asymptotic frequency of oscillations in the $x = A/\omega$ variable, given by the factor $\sin(2x)$, which therefore differs from the frequency in the old approximation (5). It also provides an explicit expression

for the amplitude of oscillations, which can be read from the above formula. A comparison between the exact W and W_{asym} is shown in fig. 2.

The minimum and maximum values of the transition rate at any oscillating period can also be read from (15):

$$W_{\text{asym}} \Big|_{\text{max}} = \frac{\Delta^2}{2x\omega} \frac{\sinh(\pi\gamma)}{\cosh(\pi\gamma) - \cos(\pi\varepsilon)}, \quad W_{\text{asym}} \Big|_{\text{min}} = \frac{\Delta^2}{2x\omega} \frac{\sinh(\pi\gamma)}{\cosh(\pi\gamma) + \cos(\pi\varepsilon)}, \quad (16)$$

where we assumed $\cos(\pi\varepsilon) > 0$. As $\cos(\pi\varepsilon)$ flips sign, all minima become maxima and viceversa.

The general formula (8) can be applied in many experimental setups involving harmonic periodic driving. Some examples will be discussed below. The asymptotic formula (15) reveals some remarkable features. To leading order in the asymptotic expansion in $1/x$, the oscillations in the x variable are multiplied by $\cos(\pi\varepsilon)$, so they vanish for the special values of ε ,

$$\varepsilon = n + \frac{1}{2}, \quad n \in \mathbb{Z},$$

giving

$$\frac{2}{x} \frac{\sinh(\pi\gamma)}{\cosh(2\pi\gamma) - \cos(2\pi\varepsilon)} (\cosh(\pi\gamma) + \cos(\pi\varepsilon) \sin(2x)) \longrightarrow \frac{1}{x} \tanh(\pi\gamma). \quad (17)$$

For such special values of the detuning parameter $\mathcal{E} = \varepsilon\omega$ there is a significant suppression in the amplitude of oscillations in x , which becomes of $O(1/x^2)$ (the residual oscillating $O(1/x^2)$ contribution originates from corrections to the asymptotic formula (12)). This is shown in fig. 3. This important property is only revealed after carrying out the exact summation over n , which may explain why it was overlooked in previous analyses.

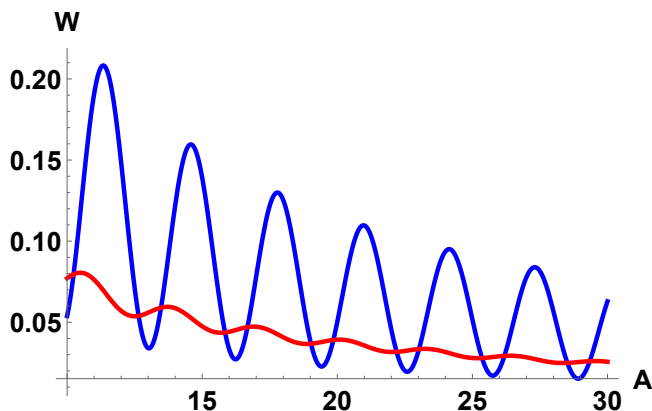


FIG. 3. The exact W given in (9) (in units of Δ^2/ω) as a function of A (in units of ω). The oscillations are strongly suppressed at half-integer values of the detuning parameter. Here $\gamma = 0.3$, $\varepsilon = 5/2$ (red) and $\varepsilon = 1.2 \times 5/2$ (blue).

Another noteworthy property of the formula (15) regards the γ dependence. For small γ and generic values of ε , the transition rate is $O(\gamma)$ due to the factor $\sinh(\pi\gamma)$. As discussed

above, the expected resonances appear for integer ε , a property that is also manifest from the asymptotic formula:

$$W_{\text{asym}} \longrightarrow \frac{\Delta^2}{2x\omega} \frac{1}{\sinh(\pi\gamma)} (\cosh(\pi\gamma) \pm \sin(2x)) \approx \frac{1}{\gamma} \frac{\Delta^2}{2\pi x\omega} (1 \pm \sin(2x)),$$

where the signs \pm correspond to even and odd ε , respectively. Thus the transition rate becomes large, $O(1/\gamma)$. An exception arises for the special values of the amplitude where $\sin(2x) = \mp 1$, resulting in the suppression of the resonance peaks. These specific values of the amplitude $A = \omega x$ correspond to the asymptotic values of the zeroes of $J_n(x)$, as previously discussed.

Note the marked change of behavior at special values of x . For generic x , the asymptotic transition rate is a periodic function of ε with period $\varepsilon = \varepsilon + 2n$. However, at the special values

$$x = \frac{n\pi}{2}, \quad n \in \mathbb{Z},$$

one has $\sin(2x) = 0$ and the period suddenly becomes $\varepsilon = \varepsilon + n$.

It would be extremely interesting to experimentally test all these distinctive features.

Finally, it is also worth looking at the behavior of W at small amplitudes. Using [21]²

$$\frac{\pi}{\sin(\pi\mu)} J_\mu(x) J_{-\mu}(x) = \frac{1}{\mu} \left(1 + \sum_{m=1}^{\infty} \frac{(2m)!}{2^{2m} (m!)^2} \frac{x^{2m}}{(\mu^2 - 1^2)(\mu^2 - 2^2) \cdots (\mu^2 - m^2)} \right), \quad (18)$$

we find

$$W(x=0) = \frac{\Delta^2 \gamma}{2\omega |\mu|^2}. \quad (19)$$

This formula is exact and encompasses the entire summation in (2). This non-vanishing value is clearly visible in fig. 1a (where $W(x=0) \cong 0.013$). This contrasts the exponentially small value inaccurately predicted by the old and commonly used approximation (4).

A number of studies extend the study of transitions to multiple energy levels and use W as building block as the transition rate between a given pair of energy levels [22–24]. This introduces of course, multiple energy bias parameters, one for each pair, and our evaluation applies directly to each W .

A. Upper-level occupation probability and Stückelberg phase

The formula (15) can also be written as

$$W_{\text{asym}} = \frac{\Delta^2}{x\omega} b \left(a - \sin^2\left(x - \frac{\pi}{2}\varepsilon - \frac{\pi}{4}\right) - \sin^2\left(x + \frac{\pi}{2}\varepsilon - \frac{\pi}{4}\right) \right), \quad (20)$$

² The formula follows from an identity in [20].

with

$$b \equiv \frac{\sinh(\pi\gamma)}{\cosh(2\pi\gamma) - \cos(2\pi\varepsilon)}, \quad a \equiv 2 \cosh^2\left(\frac{1}{2}\pi\gamma\right). \quad (21)$$

It should be noted that the oscillation frequency in the $x = A/\omega$ variable is equal to 2. This is in sharp contrast with the predicted asymptotic frequency of the approximation (4), where, for large A , it has the form (5) and predicts an incorrect frequency $\frac{4\sqrt{2}}{3} \neq 2$. As a consequence, at large x , the approximation (4) gets completely out of phase.

The above asymptotic behavior (20) can be compared with known results for the upper-level occupation probability, obtained within the adiabatic-impulse model, in the double-passage regime and in the fast passage limit $\Delta^2/(A\omega) \ll 1$ [3]. The upper-level occupation probability is the square of the absolute value of the probability amplitude and its time-average is a sum of Lorentzian-shape k -photon resonances of higher analytical complexity than the transition rate, see Eq. (55) in [2], but in the above limit, it is proportionally related to the transition rate, giving (see Appendix B4.4 in [3])

$$P_+^{\text{double}} \approx \frac{2\pi\Delta^2}{\omega A} \sin^2\left(x - \frac{\pi}{2}\varepsilon - \frac{\pi}{4}\right). \quad (22)$$

Thus we see that the asymptotic expression (20) corresponding to the exact transition rate reproduces the expected frequency and also the expected ε dependence. That is, it reproduces the Stückelberg phase.

B. Fourier transforms of the transition rate

We now compute the Fourier transforms of W in both variables \mathcal{E} and A . The characteristic function of a Lorentzian is an exponential. That is:

$$\int_{-\infty}^{\infty} \frac{\lambda e^{ixt}}{\pi(\lambda^2 + (x - x_0)^2)} dx = \exp(x_0 it - \lambda |t|).$$

We want to Fourier transform with regards to \mathcal{E} both in itself and en route to the 2d Fourier, discussed by other means in [9]. So, we consider

$$\sum_{n \in \mathbb{Z}} \frac{J_n(x)^2 \Gamma_2}{(\mathcal{E} - n\omega)^2 + \Gamma_2^2}$$

and instead of using (9) and then transform, we carry out the term by term transform (the dominated convergence theorem allows us to exchange integration and summation), then

$$\widehat{W}(k_{\mathcal{E}}, x) = \frac{\Delta^2}{2} \sum_{n \in \mathbb{Z}} \int_{-\infty}^{\infty} \frac{J_n(x)^2 \Gamma_2 e^{-i\mathcal{E}k_{\mathcal{E}}}}{(\mathcal{E} - n\omega)^2 + \Gamma_2^2} d\mathcal{E} = \frac{\pi\Delta^2}{2} \sum_{n \in \mathbb{Z}} J_n(x)^2 \exp(-n\omega i k_{\mathcal{E}} - \Gamma_2 |k_{\mathcal{E}}|). \quad (23)$$

Notice that $k_{\mathcal{E}}$ has dimension of time. The summation can be carried out. Recall Graf's addition theorem [20]:

$$\sum_{l \in \mathbb{Z}} t^l J_l(x) J_{l+m}(y) = \left(\frac{y - x/t}{y - xt} \right)^{n/2} J_m \left(\sqrt{x^2 + y^2 - xy \frac{t^2 + 1}{t}} \right).$$

It simplifies since $m = 0$ in our case:

$$\widehat{W}(k_{\mathcal{E}}, x) = \frac{\pi \Delta^2}{2} \exp(-\Gamma_2 |k_{\mathcal{E}}|) J_0 \left(\sqrt{2x^2(1 - \cos(\omega k_{\mathcal{E}}))} \right), \quad (24)$$

i.e.

$$\boxed{\widehat{W}(k_{\mathcal{E}}, x) = \frac{\pi \Delta^2}{2} \exp(-\Gamma_2 |k_{\mathcal{E}}|) J_0(2x |\sin(\omega k_{\mathcal{E}}/2)|)} \quad (25)$$

The formula shows that $\widehat{W}(k_{\mathcal{E}}, x)$ has an infinite number of zeroes in the real x axes, given by the zeroes of the Bessel function. $\widehat{W}(k_{\mathcal{E}}, x)$ exhibits an oscillatory behavior, with an amplitude modulated by the exponential factor $\exp(-\Gamma_2 |k_{\mathcal{E}}|)$. In particular, the formula (25) predicts the following oscillatory behavior at small x :

$$\widehat{W}(k_{\mathcal{E}}, x) \approx \frac{\pi \Delta^2}{2} \exp(-\Gamma_2 |k_{\mathcal{E}}|) \left(1 - x^2 \sin^2 \left(\frac{\omega k_{\mathcal{E}}}{2} \right) \right), \quad x \ll 1. \quad (26)$$

We can now look for the Fourier transform with regards to the x variable (the amplitude) using either (23) and/or (24). The route (24) seems simpler since we only have to transform $J_0(\alpha x)$ where $\alpha := 2 |\sin(\omega k_{\mathcal{E}}/2)|$ and we know that [25]:

$$\int_{-\infty}^{\infty} J_n(x) e^{-ik_x x} dx = \frac{2(-i)^n T_n(k_x)}{\sqrt{1 - k_x^2}} \text{ for } |k_x| < 1,$$

where T_n is the first degree Chebyshev polynomials (which will not appear because $n = 0$ above). Then

$$\widetilde{\widehat{W}}(k_{\mathcal{E}}, k_x) = \pi \Delta^2 \frac{\exp(-\Gamma_2 |k_{\mathcal{E}}|)}{\alpha \sqrt{1 - k_x^2/\alpha^2}} = \pi \Delta^2 \frac{\exp(-\Gamma_2 |k_{\mathcal{E}}|)}{\sqrt{2(1 - \cos(\omega k_{\mathcal{E}})) - k_x^2}}. \quad (27)$$

Recalling that $x = A/\omega$, in terms of A this reads

$$\widetilde{\widehat{W}}(k_{\mathcal{E}}, k_A) = \pi \Delta^2 \frac{\exp(-\Gamma_2 |k_{\mathcal{E}}|)}{\sqrt{\frac{4}{\omega^2} \sin^2 \left(\frac{\omega k_{\mathcal{E}}}{2} \right) - k_A^2}}. \quad (28)$$

This formula agrees with the double Fourier transform in \mathcal{E} and A given in (15) in [9]. However, here we find a new closed formula (25) for the single Fourier transform in \mathcal{E} (and, below, also for the Fourier transform in A , $\widehat{W}(\mathcal{E}, k_x)$).

1. Fourier transform in A

The other partial (1D) Fourier transform, w.r.t. the variable x can also be evaluated. The function $J_\mu(x)J_{-\mu}(x)$ is even in x , therefore (Gradshteyn, 6.672, 2. Page 719, 8th edition)

$$\widehat{W}(\mathcal{E}, k_x) = \frac{\pi}{\sin \pi \mu} \int_{-\infty}^{\infty} J_\mu(x)J_{-\mu}(x)e^{ixk_x} dx = \frac{2\pi}{\sin \pi \mu} \int_0^{\infty} J_\mu(x)J_{-\mu}(x) \cos(k_x x) dx . \quad (29)$$

Computing the integral we find

$$\widehat{W}(\mathcal{E}, k_x) = \begin{cases} \frac{\pi}{\sin \pi \mu} P_{\mu-\frac{1}{2}}\left(\frac{k_x^2}{2} - 1\right) & \text{for } 0 \leq k_x \leq 2 \\ 0 & \text{for } k_x < 0 \text{ or } k_x > 2 \end{cases} \quad (30)$$

where $P_{\mu-\frac{1}{2}}$ is the Legendre function. Thus the Fourier transform gives a compact support function: the Fourier transformed transition vanishes identically outside the interval $0 < k_x < 2$.

A version of the Paley-Wiener theorem guarantees precisely that: the Fourier transform of a function which is the real restriction of a complex entire function is a function of compact support and vice versa. The Bessel function $J_\mu(z)$ is indeed an entire function.

III. FLUORESCENCE SPECTRA OF QUANTUM DOTS

An examination of literature and reviews on Floquet physics, specifically quantum systems under external AC (harmonic) field modulation, which includes a large number of photo-assisted processes, will reveal a plethora of appearances of expressions of the type on the left-hand side of Eq. (A1). In previous studies, this expression was invariably left in summation form and customarily analyzed only numerically [26]. A prominent example is the power spectrum of fluorescence in quantum dots.

We recall that the transition rate in a modulated system is given by the Fourier transform of the stationary two-time correlation function of the Hamiltonian expressed in the interaction picture. Therefore, it is given by the power spectral density of the probe operator evaluated in the unperturbed system. Absorptive transitions in the rotating wave approximation (RWA) can be written as [26]

$$S(\omega) = \frac{g_P^2}{4} \int_{-\infty}^{\infty} e^{i\omega t} \langle \hat{\sigma}_-(t) \hat{\sigma}_+(0) \rangle dt, \quad (31)$$

where g_P represents the strength of the probe and $\hat{\sigma}_\pm$ are qubit raising and lowering operators. For harmonic modulations, this leads to the following multi-photon sideband-spectrum:

$$S(\omega) = \sum_{m=-\infty}^{\infty} \frac{g_P^2}{2} \frac{\Gamma_2 J_m^2(x)}{(\delta + m\Omega)^2 + \Gamma_2^2}, \quad (32)$$

where $\delta \equiv \omega_0 - \omega$ is the detuning between the static qubit and the probe. Thus one finds the same expression arising in the previous section in the context of superconducting qubits. Indeed, this formula controls the power spectrum in a broad class of two-level systems with harmonic driving [26, 27].

Let us now consider the setting of [14], studying InAs/GaAs quantum dots. The formula (32) reappears in the form of resolved sideband emission, due to surface acoustic waves (SAW) [14]. Indeed, some of the results in [14] are formally equivalent to the previous LZSM results. We will first present the equivalent model and subsequently discuss the effect of adding an interaction term to the Hamiltonian. This leads to a distinct application of the formula (A1).

The quantum dot (QD) is modelled as a two-level system (TLS) in [14], with electric dipole operator $\hat{d} = d\sigma_x$, and dynamics governed by the Hamiltonian

$$H = \frac{\hbar}{2} (\omega_0 + \chi\omega_s \sin(\omega_s t)) \sigma_z \quad (33)$$

and relaxation terms that cause the off-diagonal elements of the density matrix ρ to decay at a rate γ . The σ_i are Pauli matrices and the modulation index χ is a dimensionless parameter that expresses the amplitude in units of ω_s .

The fluorescence is proportional to the expectation value $\langle \hat{d}(t) \rangle = \text{Tr}(\rho(t) \hat{d})$. In the limit $\omega_s \gg 2\gamma$, where 2γ denotes the line width, one finds the following power spectrum of the fluorescence [14]

$$P[\omega] = \sum_{n=-\infty}^{\infty} \frac{J_n^2(\chi)}{\gamma^2 + (\omega - \omega_0 + n\omega_s)^2} . \quad (34)$$

Applying the summation formula (8), we find

$$P[\omega] = -\frac{1}{\gamma\omega_s} \text{Im} \left(\frac{\pi}{\sin(\pi\nu)} J_\nu(\chi) J_{-\nu}(\chi) \right) , \quad \nu = \frac{1}{\omega_s} (\omega - \omega_0 + i\gamma) . \quad (35)$$

For large χ , we can express this result in terms of trigonometric functions, as in (14), and read the frequency thereof. We get

$$P[\omega]_{\text{asym}} = \frac{2}{\chi\gamma\omega_s} b \left(\cosh\left(\frac{\pi\gamma}{\omega_s}\right) + \cos\left(\frac{\pi}{\omega_s}(\omega - \omega_0)\right) \sin(2\chi) \right) , \quad (36)$$

where now

$$b \equiv \frac{\sinh(\pi\gamma/\omega_s)}{\cosh(2\pi\gamma/\omega_s) - \cos(2\pi(\omega - \omega_0)/\omega_s)} . \quad (37)$$

The power spectrum is governed by the same formula as the transition rate in (15), with a reinterpretation of the parameters. Therefore it exhibits similar features. It has an oscillating behavior in the parameter χ , but at the special frequencies

$$\omega - \omega_0 = \omega_s \left(n + \frac{1}{2} \right) , \quad (38)$$

the oscillating behavior is suppressed by an additional factor $1/\chi$, as $\sin(2\chi)$ has vanishing coefficient in this case. As a function of ω , the asymptotic power spectrum is periodic with period $2/\omega_s$, but the period becomes $1/\omega_s$ at the special values of $\chi = n\pi/2$ where $\sin(2\chi) = 0$. On the other hand, at the resonant frequencies $\omega - \omega_0 = -n\omega_s$, the power spectrum undergoes the expected enhancement.

The experimental values in [14] for the modulation index χ are in the range $\chi \approx 0 - 2$ (see fig. 3b in [14]). The driving frequency is $\omega_s/2\pi = \nu_s = 1.05$ GHz and the linewidth is 250 MHz. It is instructive to see the changes in the fluorescence spectrum for these typical experimental values as one varies the driving frequency. Consider a resonance peak arising at $\omega - \omega_0 = -n_0\omega_s$, for some integer n_0 . Taking, for example, $n_0 = 1$, if the sum is approximated by keeping only the terms $n = n_0, n_0 \pm 1$, as compared to the exact formula, the power spectrum around this peak changes between 5 and 20 per cent, with bigger differences for larger χ . On the other hand, one can also observe the suppression of oscillations in χ occurring at half integer values of $(\omega - \omega_0)/\omega_s$ (corresponding to the minima in fig. 3a in [14]). By setting, for example, $\omega - \omega_0 = -\frac{1}{2}\omega_s$, $\omega_s/2\pi = \nu_s = 1.05$ GHz, then the oscillations in the interval $\chi = 1 - 6$ are significantly suppressed as compared with the oscillations at a generic value of $\omega - \omega_0$ (see fig. 4). This illustrates the remarkable interference effect predicted by the exact analytic formula.

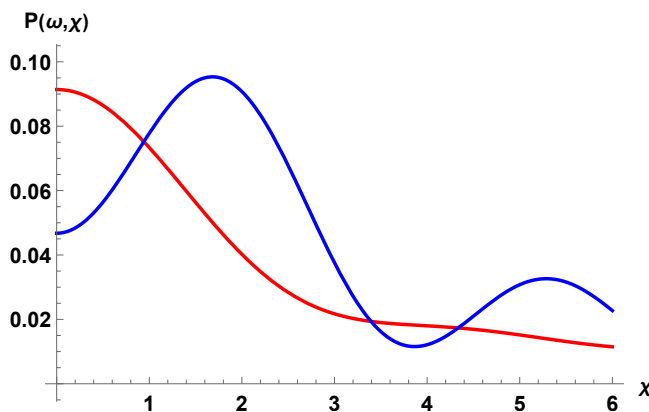


FIG. 4. The exact P given in (35) (in units of $1/\text{GHz}^2$) as a function of the dimensionless modulation index χ . The oscillations are strongly suppressed at half-integer values of $(\omega - \omega_0)/\omega_s$. Here $\gamma = 0.25$ GHz, $(\omega - \omega_0) = -\frac{1}{2}\omega_s$ (red) and $(\omega - \omega_0) = -0.7\omega_s$ (blue).

The study of quantum dots naturally prompts consideration of an area where the summation formula (A1) can have multiple applications, namely cavity optomechanics [28]. For example, it is possible to have sideband cooling of a nanomechanical resonator with an embedded QD [29], which involves the quantized transfer of energy from a mechanical mode of the resonator

to the applied optical field. This was studied with resonant spectroscopy in [14].

The coupling of the resonant laser to the two-level system is described by adding to the Hamiltonian an additional interaction term

$$H_{\text{int}} = -dE_0 \cos(\omega_L t) \sigma_x, \quad (39)$$

describing the dipole coupling of the QD to a laser field $E_0 \cos(\omega_L t)$. In [14], the power spectrum of the fluorescence for weak excitations is found to be proportional to

$$P[\omega] = \sum_{\ell=-\infty}^{\infty} \left| \sum_{n=-\infty}^{\infty} \frac{J_{\ell+n}(\chi) J_n(\chi)}{\gamma - i(\omega_L - \omega_0 + n\omega_s)} \right|^2 \delta(\omega - \omega_L + \ell\omega_s), \quad (40)$$

which can be obtained by calculating the time dependence of the atomic dipole moment in the steady state. This is of the form of a series of discrete lines at frequencies $\omega_\ell = \omega_L - \ell\omega_s$, spectrally separated from the excitation frequency by multiples of the SAW frequency. We now give an analytical evaluation of the strength of these lines.

The sum in (40) involves a novel application of the summation formula (A1), where now α or β may be different from zero. This structure will be ubiquitous in cavity optomechanics. The emission frequencies differing from the excitation frequency corresponds to the transfer of mechanical energy to the light field.

Using (A2), we find

$$\begin{aligned} \sum_{n=-\infty}^{\infty} \frac{J_{\ell+n}(z) J_n(z)}{n + \mu} &= \frac{\pi}{\sin(\pi\mu)} J_{\ell-\mu}(z) J_\mu(z), \quad \ell \geq 0, \\ \sum_{n=-\infty}^{\infty} \frac{J_{\ell+n}(z) J_n(z)}{n + \mu} &= (-1)^\ell \frac{\pi}{\sin(\pi\mu)} J_{\mu-\ell}(z) J_{-\mu}(z), \quad \ell < 0. \end{aligned} \quad (41)$$

Therefore we find

$$P[\omega] = P_+[\omega] + P_-[\omega], \quad (42)$$

where P_+ , P_- refer to the contributions from positive and negative ℓ . Respectively, they describe the two sets of frequencies of the spectrum $\omega = \omega_s \mp \ell\omega_s$. Explicitly,

$$P_+[\omega] = \frac{1}{\omega_s^2} \left| \frac{\pi}{\sin(\pi\mu)} J_\mu(\chi) \right|^2 \sum_{\ell=0}^{\infty} |J_{\ell-\mu}(\chi)|^2 \delta(\omega - \omega_L + \ell\omega_s), \quad (43)$$

$$P_-[\omega] = \frac{1}{\omega_s^2} \left| \frac{\pi}{\sin(\pi\mu)} J_{-\mu}(\chi) \right|^2 \sum_{\ell=1}^{\infty} |J_{\ell+\mu}(\chi)|^2 \delta(\omega - \omega_L - \ell\omega_s), \quad (44)$$

$$\mu = \zeta + i\eta, \quad \zeta \equiv \frac{\omega_L - \omega_0}{\omega_s}, \quad \eta \equiv \frac{\gamma}{\omega_s}. \quad (45)$$

$P_+[\omega]$ and $P_-[\omega]$ exhibit an oscillatory behavior in χ and in ζ .

For large χ , the Bessel functions can be replaced by their asymptotic expressions. Explicit formulas are given in appendix B. One can characterize the detailed features of the power spectrum and read frequencies and amplitudes thereof in terms of the physical parameters. The power spectrum has different properties in the “even” sector $\omega = \omega_L - 2k\omega_s$ and in the “odd” sector $\omega = \omega_L - (2k + 1)\omega_s$. In particular, for $\omega = \omega_L - 2k\omega_s$, $k \in \mathbb{Z}$, in the limit that the line width $\gamma \rightarrow 0$, the power spectrum takes the simple form

$$P[\omega]_{\text{even}} = \frac{(\cos(2\pi\zeta) + \sin(2\chi))^2}{\chi^2 \omega_s^2 \sin^2(\pi\zeta)} \sum_k \delta(\omega - \omega_L + 2k\omega_s). \quad (46)$$

The poles at integer ζ correspond to resonance peaks in the complete formula with $\gamma \neq 0$ (see appendix B). The height of the peak is proportional to $(1 + \sin(2\chi))^2/\chi^2$, exhibiting a $1/\chi^2$ decrease at large χ . Remarkably, for the special values

$$\chi = -\frac{\pi}{4} + \pi n, \quad n \in \mathbb{Z},$$

all resonance peaks in the detuning parameter ζ disappear (modulo $O(1/\chi^3)$ corrections). On the other hand, at the same special values of χ , $P[\omega]_{\text{odd}}$ becomes $O(1)$ instead of $O(1/\gamma^2)$ at the resonance peaks located at integer values of ζ .

Another feature is the fact that the power spectrum (46) identically vanishes at parameters satisfying $\sin(2\chi) = -\cos(2\pi\zeta)$ (more precisely, at these special values $P_{\text{even}}[\omega]$ is strongly suppressed and becomes $O(1/\chi^3)$). Similar features are shared by $P_{\text{odd}}[\omega]$.

It should be possible to test these intriguing properties in a laboratory setting.

A. Power spectrum in other QD systems

The use of Eq. (A2) is also applicable to a host of fluorescence spectra. The power spectrum is usually left in summation form (see for example [15, 16, 30]). However, it is now possible to compute all the infinite sums and provide the corresponding analytical expressions. Just as in the earlier examples, the closed formulas reveal important aspects of the physics that become manifest after resummation.

1. Coherent scattered light and atomic inversion

The spectrum of light scattered by a two-level atom in an intense laser beam with amplitude modulated light was considered long ago and just a few years after foundational works, such as

[17] and [31]. Analytical expressions already appeared in [15], in summation form, of a similar type as Eq. (40).

In [15] it was studied analytically the fluorescence spectrum in an amplitude modulated field, composed of a strong resonant component of frequency ω_0 and two considerably weaker sidebands of frequencies $\omega_0 \pm \omega_1$. It was found that the spectrum is characterized by a central component, insensitive to the presence of the modulating fields, and a series of sidebands centered about the Rabi frequency Ω_0 of the resonant field. The sidebands are located at frequencies $\Omega_0 + \omega_1 n$ for $n \in \mathbb{Z}$.

For the steady state solution $\langle \sigma_+(t) \rangle$ of the optical Bloch equations, the spectral distribution of the coherently scattered light is [15]

$$I_{\text{coh}}(\omega) \approx \frac{\pi\gamma^2}{8} \sum_{k=-\infty}^{\infty} Y_k Y_k^* \delta(\omega - \omega_L + k\omega_1),$$

where

$$Y_k \equiv \sum_{m=-\infty}^{\infty} J_m \left(\frac{a\Omega_0}{\omega_1} \right) \left(\frac{J_{m-k} \left(\frac{a\Omega_0}{\omega_1} \right)}{\frac{3}{4}\gamma - i(\Omega_0 + m\omega_1)} - \frac{J_{m+k} \left(\frac{a\Omega_0}{\omega_1} \right)}{\frac{3}{4}\gamma + i(\Omega_0 + m\omega_1)} \right). \quad (47)$$

Using (A2), we obtain

$$Y_k = \frac{i\pi}{\omega_1} \left((-1)^k \frac{J_{-\rho} J_{k+\rho}}{\sin(\pi\rho)} + \frac{J_{\rho^*} J_{k-\rho^*}}{\sin(\pi\rho^*)} \right), \quad \text{for } k \geq 0,$$

$$Y_k = \frac{i\pi}{\omega_1} \left(\frac{J_{\rho} J_{-k-\rho}}{\sin(\pi\rho)} + (-1)^k \frac{J_{-\rho^*} J_{-k+\rho^*}}{\sin(\pi\rho^*)} \right), \quad \text{for } k \leq 0,$$

where

$$\rho \equiv \frac{\Omega_0}{\omega_1} + i \frac{3\gamma}{4\omega_1}. \quad (48)$$

Therefore

$$I_{\text{coh}}(\omega) \approx \frac{\pi^3\gamma^2}{8\omega_1^2} \left(\sum_{k=0}^{\infty} a_k \delta(\omega - \omega_L + k\omega_1) + \sum_{k=-\infty}^{-1} b_k \delta(\omega - \omega_L + k\omega_1) \right),$$

with

$$a_k = \left| (-1)^k \frac{J_{-\rho} J_{k+\rho}}{\sin(\pi\rho)} + \frac{J_{\rho^*} J_{k-\rho^*}}{\sin(\pi\rho^*)} \right|^2,$$

$$b_k = \left| \frac{J_{\rho} J_{-k-\rho}}{\sin(\pi\rho)} + (-1)^k \frac{J_{-\rho^*} J_{-k+\rho^*}}{\sin(\pi\rho^*)} \right|^2.$$

Here the argument of all Bessel functions is $\frac{a\Omega_0}{\omega_1}$ as in the original expression (47). The formula now displays the explicit dependence of the spectral distribution in all physical parameters. It can be analysed in the same form as done in previous examples.

2. Steady state solutions. Atomic inversion

The steady-state atomic dipole moment $\langle \sigma_+(t) \rangle$ and inversion $\langle \sigma_z(t) \rangle$ are time-dependent and contain oscillations for all the harmonics of the modulation frequency ω_1 . The expectation value of $\langle \sigma_z(t) \rangle$ is equal to the difference between the upper-state and lower-state populations (atomic inversion), γ denotes the spontaneous decay rate of the upper level [15].

One can obtain approximate solutions of the optical Bloch equations, valid for strong driving fields at resonance ($\Omega(t) \gg \gamma^2/16$). The result is [15, 32]

$$z(t) = \langle \sigma_z(t) \rangle = -\gamma \operatorname{Re} \left(\sum_{m,k=-\infty}^{\infty} \frac{J_{m-k} \left(\frac{a\Omega_0}{\omega_1} \right) J_m \left(\frac{a\Omega_0}{\omega_1} \right) \exp(-ik\omega_1 t)}{\frac{3}{4}\gamma - i(\Omega_0 + m\omega_1)} \right)$$

and $y(t) = -2i \langle \sigma_+(t) \rangle$ is given by a similar double sum expression, with $-\gamma \operatorname{Re} \rightarrow \gamma \operatorname{Im}$ [15].

Thus, using (A2), one can now evaluate the atomic inversion term z_0 (corresponding to $k = 0$) and also any other subharmonic, for either positive or negative k . We obtain the following exact formulas for the harmonics:

$$z(t) = \sum_{k=-\infty}^{\infty} \beta_k e^{-ik\omega_1 t} \quad (49)$$

$$\begin{aligned} \beta_k &= (-1)^k \frac{\pi\gamma}{\omega_1} \operatorname{Im} \left(\frac{J_{-\rho} J_{k+\rho}}{\sin(\pi\rho)} \right), \quad \text{for } k \geq 0, \\ \beta_k &= \frac{\pi\gamma}{\omega_1} \operatorname{Im} \left(\frac{J_{\rho} J_{-k-\rho}}{\sin(\pi\rho)} \right), \quad \text{for } k < 0. \end{aligned} \quad (50)$$

The harmonics satisfy the following recurrence relations, inherited from the familiar recurrence relations of the Bessel functions,

$$\beta_{k+1} + \beta_{k-1} = -\frac{2\omega_1(k+\rho)}{a\Omega_0} \beta_k, \quad k \neq 0. \quad (51)$$

B. Asymmetric quantum dots with bi-chromatic electromagnetic field

In [16], an asymmetric quantum dot with broken inversion symmetry along the z axis together with a bi-chromatic field was considered,

$$\mathbf{E}(t) = \mathbf{E}_1 \cos \omega_1 t + \mathbf{E}_2 \cos \omega_2 t, \quad (52)$$

with $\mathbf{E}_1 = (0, 0, E_1)$, $\mathbf{E}_2 = (E_2, 0, 0)$. It was also assumed that the second frequency ω_2 was close to the electronic resonance frequency, while the first frequency ω_1 was far from resonance. The resonance condition is

$$\omega_0 \pm \omega_2 = n\omega_1, \quad (53)$$

and in [16] all modes except the resonant one are neglected. Therefore, the parameter n above, denoting the number of modes, will appear in the power spectrum below. Then

$$F_n = -(d_{12}E_2/2\hbar)J_n(\tilde{\omega}/\omega_1) \quad (54)$$

are the Rabi frequencies of the considered system and

$$\tilde{\omega} = \frac{E_1(d_{22} - d_{11})}{\hbar} \quad (55)$$

is the effective frequency, whereas $\varphi_n = \omega_0 \pm \omega_2 - n\omega_1$ is the resonance detuning. The amplitudes of the fields are E_1 and E_2 and $d_{11} = \langle 1|ez|1\rangle$, $d_{22} = \langle 2|ez|2\rangle$ and $d_{12} = d_{21} = \langle 1|ex|2\rangle$ are the matrix elements of the operator of electric dipole moment along the z, x axes, and e is the electron charge.

The problem in [16] is thus reduced to the effective two-level system driven by a monochromatic field with the combined frequency φ_n . For simplicity in the formulas, one also defines $\Omega_n = \sqrt{\frac{\varphi_n^2}{4} + F_n^2}$.

Finally, using the dressed-atom method to discuss resonant fluorescence, one finds for the width of the transitions [16]

$$\Gamma_{11} = \frac{\gamma}{2} \left(1 + \frac{\varphi_n^2}{4\Omega_n^2} \right), \quad \Gamma_{12} = \frac{\gamma}{4} \left(3 - \frac{\varphi_n^2}{4\Omega_n^2} \right). \quad (56)$$

where γ denotes the spontaneous emission rate.

The resulting inelastic power spectrum is given in terms of an infinite set of Mollow triplets [17] ($x \equiv \tilde{\omega}/\omega_1$):

$$\begin{aligned} S_2(\omega) \sim & \frac{d_{12}^2}{4\pi} \left[(1 - \Delta_S^2) \left(\frac{d_{12}E_2}{2\hbar\Omega_n} \right)^2 J_n^2(x) \sum_m \frac{J_m^2(x) \Gamma_{11}}{[\omega - (n-m)\omega_1 - \omega_2]^2 + \Gamma_{11}^2} \right. \\ & + \frac{1}{2} \frac{(1 - \varphi_n^2/4\Omega_n^2)^2}{(1 + \varphi_n^2/4\Omega_n^2)} \sum_m \left(\frac{J_m^2(x) \Gamma_{12}}{[\omega - (n-m)\omega_1 - \omega_2 + 2\Omega_n]^2 + \Gamma_{12}^2} \right. \\ & \left. \left. + \frac{J_m^2(x) \Gamma_{12}}{[\omega - (n-m)\omega_1 - \omega_2 - 2\Omega_n]^2 + \Gamma_{12}^2} \right) \right]. \quad (57) \end{aligned}$$

The infinite sums can now be carried out using our summation formula (8), giving

$$\begin{aligned} S_2(\omega) \sim & -\frac{d_{12}^2}{4\pi\omega_1} \left[(1 - \Delta_S^2) \left(\frac{d_{12}E_2}{2\hbar\Omega_n} \right)^2 J_n^2(x) \operatorname{Im} \left(\frac{\pi}{\sin(\pi\nu_1)} J_{\nu_1}(x) J_{-\nu_1}(x) \right) \right. \\ & \left. + \frac{(1 - \varphi_n^2/4\Omega_n^2)^2}{2(1 + \varphi_n^2/4\Omega_n^2)} \operatorname{Im} \left(\frac{\pi}{\sin(\pi\nu_2)} J_{\nu_2}(x) J_{-\nu_2}(x) + \frac{\pi}{\sin(\pi\nu_3)} J_{\nu_3}(x) J_{-\nu_3}(x) \right) \right]. \quad (58) \end{aligned}$$

where the spectral parameters of the Bessel functions are:

$$\begin{aligned}\nu_1 &= n + \frac{1}{\omega_1} (\omega_2 - \omega + i\Gamma_{11}), \\ \nu_2 &= n + \frac{1}{\omega_1} (\omega_2 - \omega - 2\Omega_n + i\Gamma_{12}), \\ \nu_3 &= n + \frac{1}{\omega_1} (\omega_2 - \omega + 2\Omega_n + i\Gamma_{12}).\end{aligned}$$

IV. CONCLUDING REMARKS

Sideband multiphoton spectra similar to (2), (40), (57) are ubiquitous in two-level systems with harmonic modulation. In this paper we provided exact formulas that compute the infinite sums, enabling exploration of different spectra across all parameter space.

In Section II we have seen that the transition rate is an oscillating function of the driving field amplitude that never vanishes. At large amplitude the exact transition rate can be written in terms of trigonometric functions, providing simple expressions to test a number of features. In particular, one interesting feature is the suppression of these oscillations for half-integer values of the detuning.

As a function of the detuning parameter – represented by \mathcal{E} in section II – the transition rate exhibits the expected resonance peaks at integer \mathcal{E} . We also noticed a significant change of behavior when x is an integer multiple of $\pi/2$, where the shape of the spectrum simplifies and the period is halved. We have also analytically determined the minimum and maximum values for each period of oscillations in (16).

Analogous properties were identified in the absorption spectra of quantum dots in section III, where we also considered coupling to a more general configuration of driving fields. This includes either the addition of an extra field or the consideration of bichromatic fields. In these cases, the required summation formula appears in a different form, exploiting other particular instances of the analytical expression (A2), beyond the one employed in section II. In all cases, closed formulas for the various spectra are obtained, which display explicit dependence on all physical parameters. Clearly, it would be worthwhile to conduct experiments to test the properties predicted by the analytical formulas in superconducting qubits or quantum dot devices.

ACKNOWLEDGEMENTS

We thank David Pérez-García and Sergio Valenzuela for useful comments. J.G.R. acknowledges financial support from grants 2021-SGR-249 (Generalitat de Catalunya) and MINECO PID2019-105614GB-C21. M.T. acknowledges financial support from FEI-EU-22-06, funded by Universidad Complutense de Madrid, and grant PID2020-113523GB-I00, funded by the Spanish Ministry of Science and Innovation. This work is financially supported by the Ministry of Economic Affairs and Digital Transformation of the Spanish Government through the QUANTUM ENIA project call - Quantum Spain project, by the European Union through the Recovery, Transformation and Resilience Plan - NextGenerationEU within the framework of the Digital Spain 2026 Agenda.

Appendix A: The summation formula

The more general form of the summation formula, found in [19], is

$$\sum_{n=-\infty}^{\infty} \frac{(-1)^n J_{\alpha+\gamma n}(z) J_{\beta-\gamma n}(x)}{n+\mu} = \frac{\pi}{\sin(\pi\mu)} J_{\alpha-\gamma\mu}(x) J_{\beta+\gamma\mu}(x), \quad (\text{A1})$$

where $\mu \in \mathbb{C}/\mathbb{Z}$, $\alpha, \beta, x \in \mathbb{C}$, $\gamma \in (0, 1]$, and $\Re(\alpha + \beta) > -1$. It is useful to explicitly quote the particular case where $\gamma = 1$, and $\alpha = p$, $\beta = q$, with $p, q \in \mathbb{Z}$, since this case frequently arises in various fluorescence spectra. The formula takes the form

$$\boxed{\sum_{n=-\infty}^{\infty} \frac{J_{n+p}(z) J_{n-q}(x)}{n+\mu} = (-1)^q \frac{\pi}{\sin(\pi\mu)} J_{p-\mu}(x) J_{q+\mu}(x)} \quad (\text{A2})$$

where we used $J_{-n}(x) = (-1)^n J_n(x)$ and convergence now requires $p + q > -1$.

Here we provide a simple proof in the case $\alpha = \beta = 0$ and $\gamma = 1$, referring to [19] for the general case. Interestingly, the product of two Bessel functions admit different integral representations [20] in terms of the integration of a single Bessel function and an additional simple trigonometric or hyperbolic function. One of these representations is called of Nicholson type,

$$J_n(x) J_{-n}(x) = \frac{2}{\pi} \int_0^{\frac{\pi}{2}} J_0(2x \cos \theta) \cos(2n\theta) d\theta. \quad (\text{A3})$$

The Bessel function in the integrand is now independent of the summation index. Therefore, the summation only involves the cos term. The simple nature of the formula and of its derivation lies in the fact that the result of the summation

$$\sum_{n=-\infty}^{\infty} \frac{(-1)^n \cos n\phi}{n+\mu} = \frac{\pi \cos \mu\phi}{\sin \pi\mu}, \quad (\text{A4})$$

where $\phi \in [-\pi, \pi]$, which is satisfied in our case, does not modify the analytical form of the integrand, because the r.h.s. of (A4) also has a cosine with the integration variable. Therefore, the resulting integral expression after the summation has the same integral representation of the product of two Bessel functions³. Therefore,

$$\begin{aligned} \sum_{n=-\infty}^{\infty} \frac{J_n(x) J_n(x)}{n + \mu} &= \frac{2}{\sin \pi \mu} \int_0^{\pi/2} J_0(2x \cos \theta) \cos(2\mu\theta) d\theta \\ &= \frac{\pi J_\mu(x) J_{-\mu}(x)}{\sin \pi \mu}. \end{aligned} \quad (\text{A5})$$

One of the first appearances, with a proof, of this formula is in [21]. The very first reference we could trace is actually [33]. This formula was rediscovered by Newberger [19], who also generalized it in the form (A1).

Appendix B: Asymptotic formulas for fluorescence spectrum

For large χ , one can again use the asymptotic formula for the Bessel function, giving

$$P[\omega] \approx P[\omega]_{\text{asym}} = P[\omega]_{\text{even}} + P_+[\omega]_{\text{odd}} + P_-[\omega]_{\text{odd}}, \quad (\text{B1})$$

with

$$\begin{aligned} P[\omega]_{\text{even}} &= \frac{4}{\chi^2 \omega_s^2} \frac{|\cos(\chi - \mu \frac{\pi}{2} - \frac{\pi}{4})|^2 |\cos(\chi + \mu \frac{\pi}{2} - \frac{\pi}{4})|^2}{|\sin(\pi \mu)|^2} \sum_k \delta(\omega - \omega_L + 2k\omega_s), \\ P_+[\omega]_{\text{odd}} &= \frac{4}{\chi^2 \omega_s^2} \frac{|\cos(\chi - \mu \frac{\pi}{2} - \frac{\pi}{4})|^2 |\sin(\chi + \mu \frac{\pi}{2} - \frac{\pi}{4})|^2}{|\sin(\pi \mu)|^2} \sum_{k=0}^{\infty} \delta(\omega - \omega_L + (2k+1)\omega_s), \\ P_-[\omega]_{\text{odd}} &= \frac{4}{\chi^2 \omega_s^2} \frac{|\cos(\chi + \mu \frac{\pi}{2} - \frac{\pi}{4})|^2 |\sin(\chi - \mu \frac{\pi}{2} - \frac{\pi}{4})|^2}{|\sin(\pi \mu)|^2} \sum_{k=0}^{\infty} \delta(\omega - \omega_L - (2k+1)\omega_s). \end{aligned}$$

Computing the modulus, we find

$$\begin{aligned} P[\omega]_{\text{even}} &= \frac{(\cosh(2\pi\eta) \cos(2\pi\zeta) + \sin(2\chi))^2 + \sin^2(2\pi\zeta) \sinh^2(2\pi\eta)}{\chi^2 \omega_s^2 (\sin^2(\pi\zeta) + \sinh^2(\pi\eta))} \sum_k \delta(\omega - \omega_L + 2k\omega_s), \\ P_+[\omega]_{\text{odd}} &= \frac{(\cosh(2\pi\eta) \sin(2\pi\zeta) - \cos(2\chi))^2 + \cos^2(2\pi\zeta) \sinh^2(2\pi\eta)}{\chi^2 \omega_s^2 (\sin^2(\pi\zeta) + \sinh^2(\pi\eta))} \sum_{k=0}^{\infty} \delta(\omega - \omega_L + (2k+1)\omega_s), \\ P_-[\omega]_{\text{odd}} &= \frac{(\cosh(2\pi\eta) \sin(2\pi\zeta) + \cos(2\chi))^2 + \cos^2(2\pi\zeta) \sinh^2(2\pi\eta)}{\chi^2 \omega_s^2 (\sin^2(\pi\zeta) + \sinh^2(\pi\eta))} \sum_{k=0}^{\infty} \delta(\omega - \omega_L - (2k+1)\omega_s). \end{aligned}$$

[1] P. Krantz, M. Kjaergaard, F. Yan, T. P. Orlando, S. Gustavsson, and W. D. Oliver, A quantum engineer's guide to superconducting qubits, *Applied physics reviews* **6** (2019).

³ The integral representation (A3) holds the same way for more general indices, including complex.

- [2] S. N. Shevchenko, S. Ashhab, and F. Nori, Landau–zener–stückelberg interferometry, *Physics Reports* **492**, 1 (2010).
- [3] V. Ivakhnenko, S. N. Shevchenko, and F. Nori, Nonadiabatic landau–zener–stückelberg–majorana transitions, dynamics, and interference, *Physics Reports* **995**, 1 (2023).
- [4] F. Di Giacomo and E. E. Nikitin, The majorana formula and the landau–zener–stückelberg treatment of the avoided crossing problem, *Physics-Uspekhi* **48**, 515 (2005).
- [5] P. O. Kofman, O. V. Ivakhnenko, S. N. Shevchenko, and F. Nori, Majorana’s approach to nonadiabatic transitions validates the adiabatic-impulse approximation, *Scientific Reports* **13**, 5053 (2023).
- [6] E. Nikitin, Nonadiabatic transitions: What we learned from old masters and how much we owe them, *Annual review of physical chemistry* **50**, 1 (1999).
- [7] D. Berns, W. Oliver, S. Valenzuela, A. Shytov, K. Berggren, L. Levitov, and T. Orlando, Coherent quasiclassical dynamics of a persistent current qubit, *Physical review letters* **97**, 150502 (2006).
- [8] W. D. Oliver, Y. Yu, J. C. Lee, K. K. Berggren, L. S. Levitov, and T. P. Orlando, Mach-zehnder interferometry in a strongly driven superconducting qubit, *Science* **310**, 1653 (2005).
- [9] M. S. Rudner, A. Shytov, L. S. Levitov, D. M. Berns, W. D. Oliver, S. O. Valenzuela, and T. P. Orlando, Quantum phase tomography of a strongly driven qubit, *Physical review letters* **101**, 190502 (2008).
- [10] J. Li, M. Silveri, K. Kumar, J.-M. Pirkkalainen, A. Vepsäläinen, W. Chien, J. Tuorila, M. Silanpää, P. Hakonen, E. Thuneberg, *et al.*, Motional averaging in a superconducting qubit, *Nature communications* **4**, 1420 (2013).
- [11] Y. Gefen, E. Ben-Jacob, and A. O. Caldeira, Zener transitions in dissipative driven systems, *Physical Review B* **36**, 2770 (1987).
- [12] E. Shimshoni and Y. Gefen, Onset of dissipation in zener dynamics: relaxation versus dephasing, *Annals of Physics* **210**, 16 (1991).
- [13] Y. Gefen and D. Thouless, Zener transitions and energy dissipation in small driven systems, *Physical review letters* **59**, 1752 (1987).
- [14] M. Metcalfe, S. M. Carr, A. Muller, G. S. Solomon, and J. Lawall, Resolved sideband emission of inas/gaas quantum dots strained by surface acoustic waves, *Physical review letters* **105**, 037401 (2010).
- [15] B. Blind, P. Fontana, and P. Thomann, Resonance fluorescence spectrum of intense amplitude modulated laser light, *Journal of Physics B: Atomic and Molecular Physics* **13**, 2717 (1980).

- [16] G. Y. Kryuchkyan, V. Shahnazaryan, O. V. Kibis, and I. Shelykh, Resonance fluorescence from an asymmetric quantum dot dressed by a bichromatic electromagnetic field, *Physical Review A* **95**, 013834 (2017).
- [17] B. Mollow, Power spectrum of light scattered by two-level systems, *Physical Review* **188** (1969).
- [18] R. M. Otxoa, A. Chatterjee, S. N. Shevchenko, S. Barraud, F. Nori, and M. F. Gonzalez-Zalba, Quantum interference capacitor based on double-passage landau-zenner-stückelberg-majorana interferometry, *Physical Review B* **100**, 205425 (2019).
- [19] B. S. Newberger, New sum rule for products of bessel functions with application to plasma physics, *Journal of Mathematical Physics* **23**, 1278 (1982).
- [20] G. N. Watson, *A treatise on the theory of Bessel functions*, Vol. 2 (The University Press, 1922).
- [21] L. S. Hall, W. Heckrotte, and T. Kammash, Ion cyclotron electrostatic instabilities, *Physical Review* **139**, A1117 (1965).
- [22] X. Wen and Y. Yu, Landau-zenner interference in multilevel superconducting flux qubits driven by large-amplitude fields, *Physical Review B* **79**, 094529 (2009).
- [23] M. Liul, A. Ryzhov, and S. Shevchenko, Interferometry of multi-level systems: rate-equation approach for a charge qudit, *The European Physical Journal Special Topics* , 1 (2023).
- [24] M. Liul and S. Shevchenko, Rate-equation approach for multi-level quantum systems, *Low Temperature Physics* **49**, 96 (2023).
- [25] H. O. Beća, An orthogonal set based on bessel functions of the first kind/skup ortogonalnih funkcija zasnovan na beselovim funkcijama prve vrste, *Publikacije Elektrotehničkog fakulteta. Serija Matematika i fizika* , 85 (1980).
- [26] M. Silveri, J. Tuorila, E. Thuneberg, and G. Paraoanu, Quantum systems under frequency modulation, *Reports on Progress in Physics* **80**, 056002 (2017).
- [27] M. Silveri, K. Kumar, J. Tuorila, J. Li, A. Vepsäläinen, E. Thuneberg, and G. Paraoanu, Stückelberg interference in a superconducting qubit under periodic latching modulation, *New Journal of Physics* **17**, 043058 (2015).
- [28] M. Aspelmeyer, T. J. Kippenberg, and F. Marquardt, Cavity optomechanics, *Reviews of Modern Physics* **86**, 1391 (2014).
- [29] I. Wilson-Rae, P. Zoller, and A. Imamoglu, Laser cooling of a nanomechanical resonator mode to its quantum ground state, *Physical review letters* **92**, 075507 (2004).
- [30] Z. Ficek, J. Seke, A. Soldatov, and G. Adam, Fluorescence spectrum of a two-level atom driven by a multiple modulated field, *Physical Review A* **64**, 013813 (2001).

- [31] C. Cohen-Tannoudji, Frontiers in laser spectroscopy, in *Proc. 27th Les Houches Summer School* (North-Holland Amsterdam, 1977) p. 3.
- [32] P. Thomann, Optical resonances in a strong modulated laser beam, *Journal of Physics B: Atomic and Molecular Physics* **13**, 1111 (1980).
- [33] H. K. Sen, Solar enhanced radiation and plasma oscillations, *Physical Review* **88**, 816 (1952).